Iraqi Journal of Physics, 2026
https://doi.org/10.30723/ijp.v24i1.1379

Vol.24, No.1, PP.55-64
P-ISSN: 2070-4003
E-ISSN: 2664-5548

Design and Implementation of a Patch Antenna Mobile Devices Treated Using Nd:YAG Laser to Improve Its Performance for Wireless Links

Sarah Y. Khoudair[1*] and Ali H. Khidhir[1]
[1]*Department of Physics, College of Science, University of Baghdad, Baghdad, Iraq*
[*]Corresponding author: alihassan1990@sc.uobaghdad.edu.iq

Abstract

This paper presents the design and implementation of an E-shaped microstrip patch antenna for wireless communication. The antenna features several advantages, including low volume, low profile, easy mounting, lightweight construction, and low fabrication cost. It operates at 3.2 and 3.4 GHz, using an FR4 substrate with a dielectric constant of 4.3 and a thickness of 1.4 mm. The design incorporates two parallel slots to perturb the surface current patch. The E-shaped antenna achieves return losses of -13 dB and -16 dB at the operating frequencies of 3.2 and 3.4 GHz, respectively. The design and simulation were conducted using CST software, with coaxial probe feeding employed. Furthermore, this study investigates the effect of surface roughness on the absorption of the radiation line of the implemented antenna, which was treated using a Nd:YAG laser by bombarding the radiation line of the desired antenna in order to gradually reduce the surface roughness, as this improved the work performance of the antenna at the resonant frequencies of 3.2 and 3.4 GHz. After treatment, the antenna exhibited return losses of -15.7 dB and -20 dB at 3.2 and 3.4 GHz, respectively. These qualities highlight the potential of the Nd:YAG laser-treated inverted E-shaped antenna for enhancing the performance of wireless communication systems.

Article Info.

Keywords:
E-shaped Patch Antenna, Bluetooth, Nd: YAG Laser, 5G, Bandwidth.

Article history:
Received: Oct. 08, 2025
Revised: Feb. 24, 2025
Accepted:Mar. 03, 2025
Published:Mar.01,2026

1. Introduction

The development of antennas has advanced rapidly in many applications, including military, commercial, medical, and telecommunications. The extensive utilization of online video streaming and multimedia devices has driven the need for increased bandwidth and gain in wireless networking. While the refinement of 4G technology is ongoing, the current emphasis lies on the advancement of 5G communication technologies. Microstrip patch antennas are widely used for their many advantages such as lightweight, small size, low manufacturing cost and ability to double operation at higher frequencies[1]. Microstrip antennas received great attention in the early 1970s, although micro-antennas can be traced back to 1953 [2].

Recently, patch antennas have become widely applicable in many communications systems. Important applications are wireless communication systems (1.8 GHz - 5.6 GHz)[3]. Despite the many advantages of patch antennas and their uses in many daily applications, they exhibit some limitations, such as low bandwidth and gain[4-6]. Therefore, many papers have reported several techniques to reduce these drawbacks, especially in widening the impedance bandwidth. Such change involves incising slots to the basic forms, changing the geometry form configuration [7, 8], or using multi-layer techniques [9]. The efficiency of the inverted E-shaped antenna can be enhanced through recent improvements by employing laser processing. Laser technology utilizes coherent light to alter the antenna's material properties and shape.

These factors can improve surface roughness, increase conductivity, and enhance

dielectric characteristics, contributing to higher antenna performance [10, 14]. By accurately manipulating the laser characteristics, it becomes possible to make customized modifications that meet specific design criteria, resulting in antennas with increased gain and broader bandwidths [15-17]. Recent developments include utilizing a Neodymium-doped Yttrium Aluminum Garnet (Nd: YAG) laser to improve antenna gain and bandwidth [17, 21]. The laser treatment accurately alters the surface and structural features of the antenna, resulting in notable enhancements in electromagnetic performance by correcting its physical and microstructural characteristics.

In this work, an inverted E-shaped patch antenna was designed and implemented. After implementing the ported antenna, the radiation line of the desired antenna was bombarded with Nd-YAG laser in order to treat the surfaces, improve the desired antenna's gain and bandwidth, and operate at frequencies from 3.2 GHz to 3.4 GHz. This technology provides a means to achieve desirable improvements in antenna properties, facilitating the advancement of more efficient wireless networks[22]. The development of micro- and nanoscale surface systems has emerged as widespread in science and technology because of improved electrical, thermal, radiative, and tribological properties in materials [23-28].

2. Antenna Design

The orientation of the presented design was inverted; Fig. 1 (a-d) shows both superior and inferior views of the constructed prototype of the E-shaped patch antenna. This paper introduces the fundamental information to design E-shaped patch antennas with operating frequencies of 3.2 and 3.4 GHz. To develop E-shaped microstrip patch antennas, the substrate was chosen to have a dielectric constant of ε_r = 4.3 and a thickness (h) of 1.4mm.

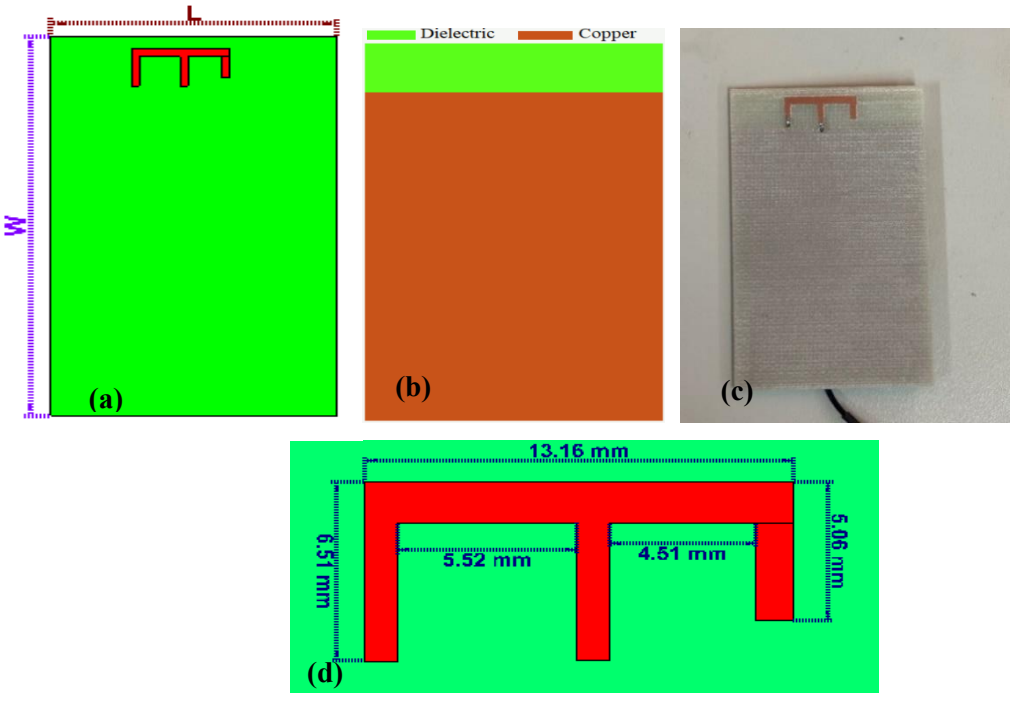

Figure 1: Configuration of the proposed antenna (a) Superior view (b) Inferior view (c) Prototype methodology and (d) Enlarged structure with sizes in millimeters.

The implementation that identifies the critical characteristics is explained using the transmission line model [28-33].

Step 1: Determination of the patch width (W)

For an electrically thin strip, the width of the microstrip patch antenna is given by Eq. (1):

$$W = \frac{c}{2f_o}\sqrt{\frac{2}{\varepsilon_r+1}} \quad (1)$$

where f_o is the resonance frequency in GHz, c is the speed of light, and ε_r is the relative permittivity of the substrate.

Step 2: Calculation of the effective dielectric constant ($\varepsilon_{\text{reff}}$), which is done using the following Eq. (2):

$$\varepsilon_{reff} = \frac{\varepsilon_r+1}{2} + \frac{\varepsilon_r-1}{2}\left(1+12\frac{h}{w}\right)^{-\frac{1}{2}} \quad (2)$$

where h is the substrate thickness.

Step 3: Calculation of the effective length (L_{eff}), Eq. (3):

$$L_{eff} = \frac{c}{2f_o\sqrt{\varepsilon_{reff}}} \quad (3)$$

Step 4: Calculation of the length extension (ΔL) through the given Eq. (4):

$$\Delta L = 0.412h\frac{(\varepsilon_{reff}+0.3)\left(\frac{w}{h}+0.264\right)}{(\varepsilon_{reff}-0.258)\left(\frac{w}{h}+0.8\right)} \quad (4)$$

Calculation of the precise patch length (La), Eq. (5):

$$La = L_{\text{eff}} - 2\Delta L \quad (5)$$

3. Results and Discussion

3.1. S-Parameters

The reflection coefficient of the fabricated antenna was simulated, as depicted in Fig. 2, with resonant frequencies of 3.2 and 3.4 GHz and then analyzed with the Site Master (Anritsu S362E). The simulated and measured data of reflection coefficient (S11) were compared as shown in Fig. 3(a-b). The S11 parameter value was less than -10 dB at 3.2 and 3.4GHz. The bandwidth was 390 MHz at 3.2 GHz and 566 MHz at 3.4 GHz. The measured results were close to the simulated results, though there was a shift, due to the fabrication tolerances and soldering losses.

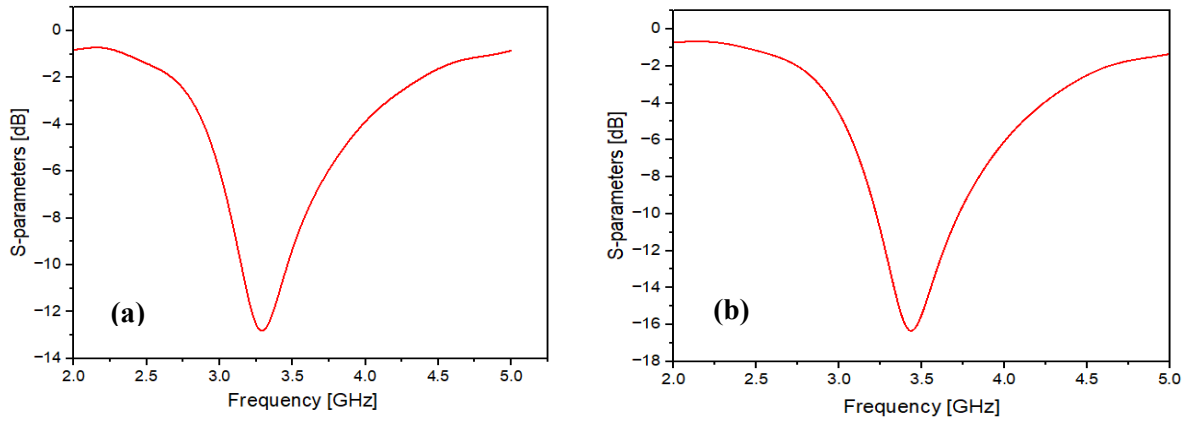

Figure 2: Simulated reflection coefficients (S11) at (a) 3.2 GHz and (b) 3.4 GHz.

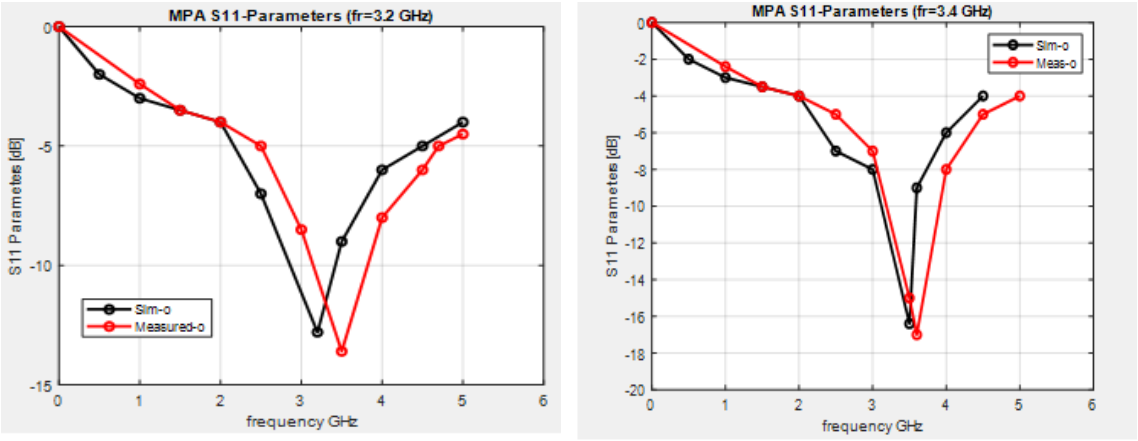

(a) (b)

Figure 3: Simulated and measured S11: (a) at 3.2 GHz and (b) at 3.4 GHz

The Voltage Standing Wave Ratio (VSWR) and characteristic impedances of transmission lines are two main factors that create the proposed design features. VSWR quantifies the power capability in radio frequency from a power supply to a load through the transmission line. Impedance matching in the RF systems is measured using the proportion of maximum to minimum amplitude of the standing wave. VSWR of 1:1 signifies impeccable alignment, minimizing reflections, and power dissipation. Characteristics impedance is defined as the ratio of voltage magnitude to current in any RF transmission line, usually 50 ohms. It describes the relationship between the voltage and current of one propagating wave.

The VSWR and impedance of the two resonance frequencies, 3.2 and 3.4 GHz, are shown in Fig. 4(a-b). The VSWR values for both cases are greater than 1, demonstrating good power transmission efficiency; the impedance values are close to 50 ohms, demonstrating good impedance matching.

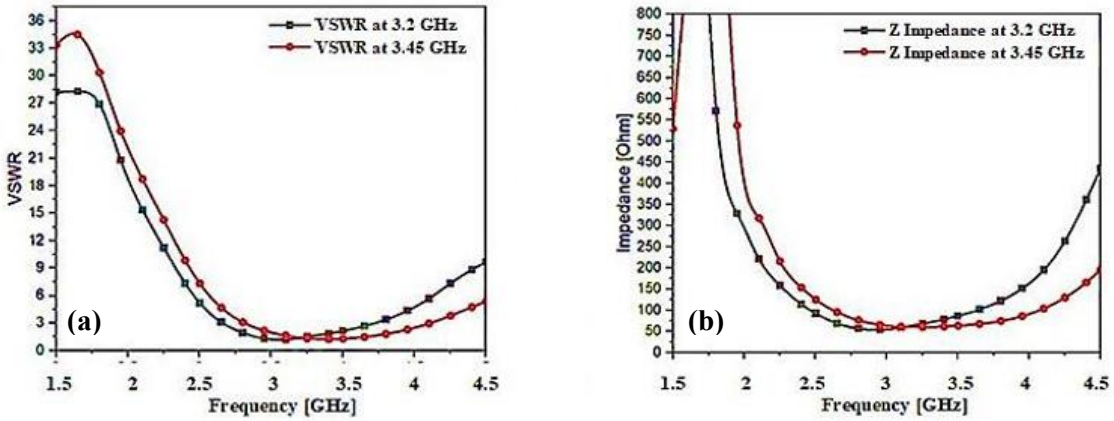

Figure 4: VSWR and characteristics impedance

3.2. Particle and Roughness Analysis

Before utilizing the Nd:YAG laser on the microstructure of the inverted E-shaped patch antenna installed on an FR-4 dielectric substrate revealed that the surface contained very little particulate matter. The particles were very small, varying between (5-150 nm), as illustrated in Fig. 5(a-b). The standard roughness measurement from Fig. 6 (a-b) was made using Atomic Force Microscopy (AFM). The results showed that surface roughness parameters were of low values.

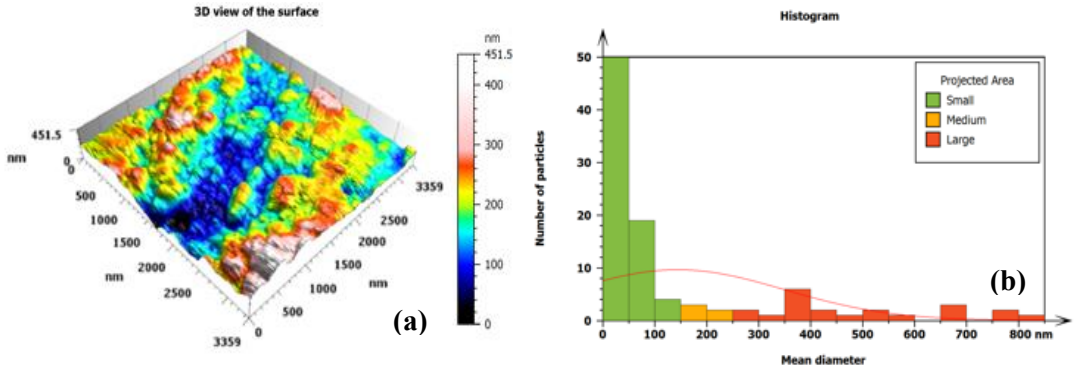

Figure 5: Particle analysis before Nd: YAG laser treatment: (a) Microstructure of E-shaped patch antenna at fr=3.4 GHz, and (b)Particles mean diameter histogram.

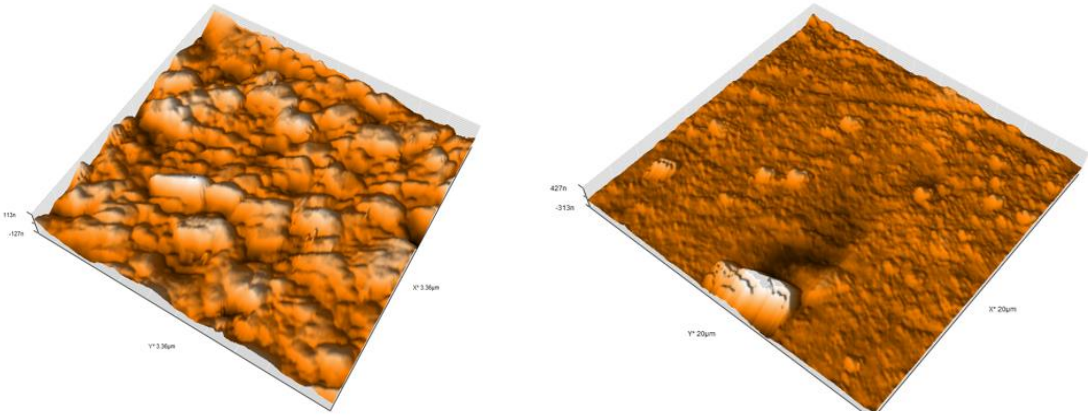

Figure 6: Surface roughness: (a) Before Nd: YAG laser treatment and (b) After at 3.4 GHz.

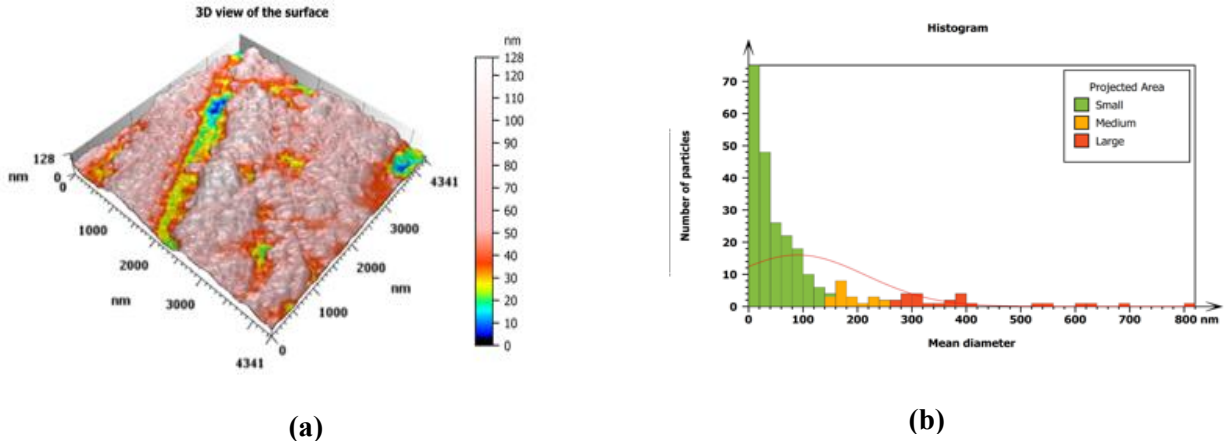

Figure 7: Particle analysis after Nd: YAG laser treatment: (a) Microstructure of E-shaped patch antenna at fr=3.4 GHz and (b) Particles mean diameter histogram.

After applying the Nd:YAG laser, significant changes in the structure of the antenna surface were observed. The topic is the final analysis of the laser ablation process and its impact on reducing the geometric surface profile parameters, including such features as crater, ridge, etc. This is brought by the collapsing of the material

through the stages of melting, vaporization and re-solidification, forming the observed geometry as shown in Fig. 7 (a-b). The surface showed irregular particle size and particle distribution because vaporized material results in debris particles that differ in size. Analysis of roughness, as presented in Fig. 6(a-b), suggests that the surface roughness parameters, including Ra and Rq were slightly reduced after the laser treatment. This may indicate that the surface became smooth, with few peaks, valleys and the overall roughness, as shown in Fig. 6 (a-b). The decrease in surface roughness impacts the characteristics of the material, such as its conductive layers and dielectric properties, because it alters the surface structure.

The differences between the measured and simulated results of the proposed antenna with and without treatment are shown in Fig. 8. The antenna provides a broad frequency range of 390 MHz and 566 MHz without any modifications and has a resonance frequency of 3.2 and 3.4 GHz. It has a response at 3.2 GHz and 3.4 GHz, as presented in Fig. 8. The measured and simulated results of the proposed antenna, both with and without treatment, exhibit a high level of agreement.

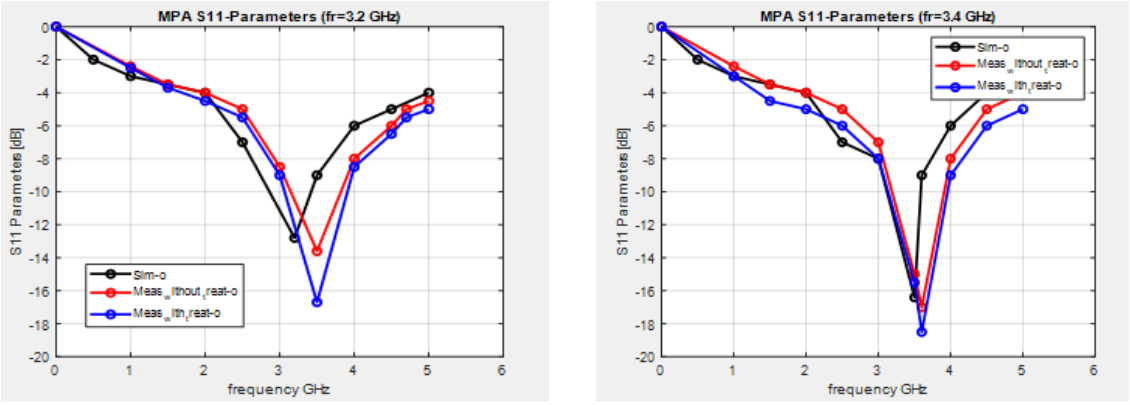

(a) **(b)**

Figure 8: Reflection coefficient with and without treatment: (a) simulated (b) measured without and with treatment

3.3. Radiation Pattern

Fig. 9 shows the radiation patterns of the three-dimensional electric field at the two frequencies, 3.2 GHz and 3.4 GHz. The magnitude of the E-field pattern was 17.2 V/m, corresponding to a peak gain of 3.2 dBi. Fig. 10 depicts the radiation pattern of the recommended E-shaped antenna in two dimensions at resonance frequencies of 3.2 GHz and 3.4 GHz without any treatment. The antenna design allows for bidirectional radiation in the E-plane at both frequencies and omnidirectional radiation in the H-plane at both operational frequencies. The radiation pattern exhibits a butterfly-shaped configuration, preferable for the electric field (E-field).

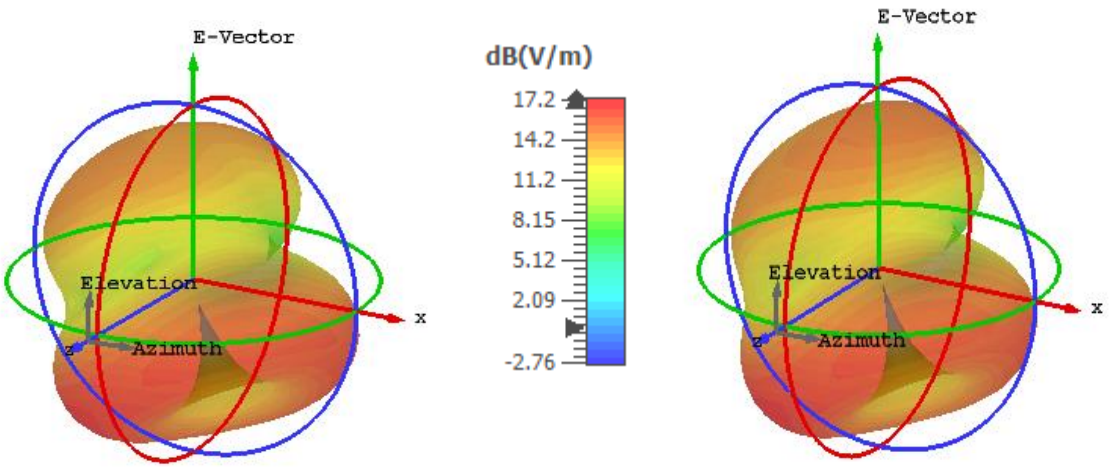

(a) **(b)**

Figure 9: 3-D radiation pattern at two frequencies at : (a) 3.2 GHz and (b) 3.4 GHz.

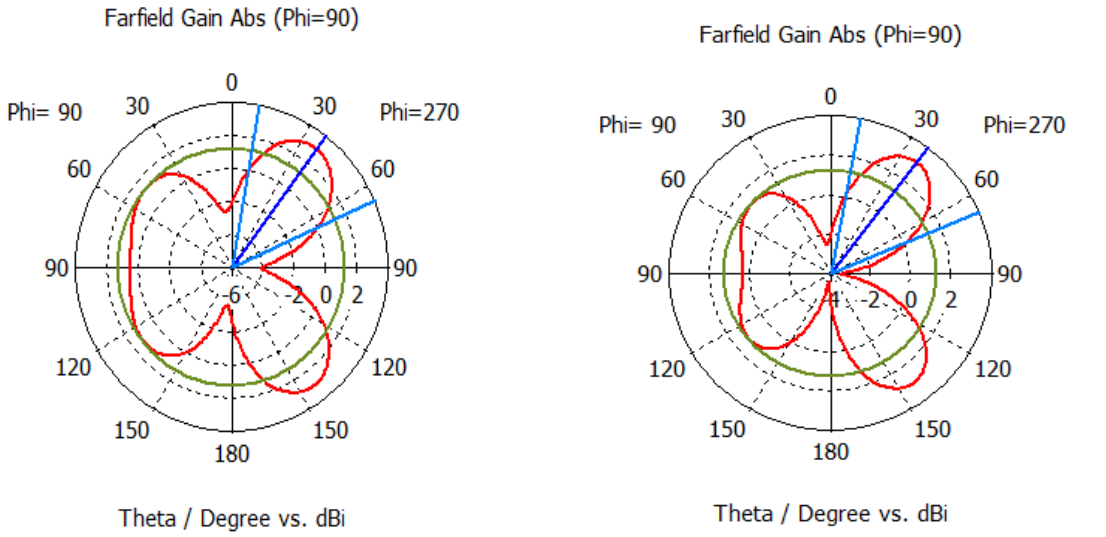

(a) **(b)**

Figure 10: 2-D electric and magnetic fields at (a) 3.2 GHz and (b) 3.4 GHz

4. Comparison with Previous Works

Table 1 compares the results of the proposed work with that of some references. The results demonstrated that the suggested configuration provided higher performance. The present design exhibited a wide frequency range 390 and 566MHz, high efficiency (over 88%), high gain (>3 dBi), impedance matching near 50 Ohms, and a compact form factor of (6.5 x 13.16 mm²); all of which are comparable to the results reported in the mentioned references. Furthermore, the VSWR value was around 1, as depicted in Fig. 4, suggesting little reflected waves and a virtually perfect match in the transmission line.

Table 1: Comparison between the proposed work and the references under consideration.

Ref. No.	Antenna size (mm^2)	Frequency (GHz)	Bandwidth (MHz)	Gain (dBi)	Eff. (%)
[26]	50 x 80	2.55 and 3.5	2920	2.5 and 3.05	N. M
[27]	28 x 20	3.65	700	2.5	
[28]	20 x 35	3.12	2560	2.44	90
[29]	36 x 37	3.45 and 5.9	160 and 220	3.8 and 0.53	59
This work	6.5 x 13.16	3.2 and 3.4	390, 566, 684	3.2 and 4.2	95

5. Conclusions

This article effectively developed and implemented an inverted E-shaped antenna that operates at 3.2 and 3.4 GHz. The antenna's performance was improved by Nd:YAG laser treatment. The results show substantial enhancements in bandwidth and gain, with initial bandwidths of 390 MHz and 566 MHz and a bandwidth of 684 MHz after treatment. The measured and calculated reflection coefficients showed |S11| values below -10 dB across the desired frequency ranges, verifying the design's and treatment's efficiency. The utilization of the Nd: YAG laser treatment has demonstrated its effectiveness in enhancing antenna performance, enabling precise manipulation of material and geometric characteristics. This approach improves the antenna's physical characteristics and provides advantageous microstructural modifications, enhancing operational efficiency. The minor discrepancies between the measured and simulated outcomes provide additional confirmation of the durability and effectiveness of the proposed design.

Conflict of Interest

Authors declare that they have no conflict of interest.

References

1. M. A. Jensen and J. W. Wallace, *IEEE Transactions on Antennas and Propagation*, **52**, 2810 (2004). https://doi.org/10.1109/TAP.2004.835272.
2. I. Locher, Ph.D. thesis (ETH Zurich, Germany) 2006. https://doi.org/10.3929/ethz-a-005135763.
3. H. Eskelinen, P. Eskelinen, and K. Tiihonen, *In 2000 30th European Microwave Conference,* October 2000. Paris, France. https://doi.org/10.1109/EUMA.2000.338879.
4. O. Leisten, J. Fieret, I.S. Boehlen, P.T. Rumsby, P. McEvoy, and Y. Vardaxoglou*, In Photon Processing in Microelectronics and Photonics*, (USA, June 2002) p. 397. https://doi.org/10.1117/12.470647.
5. D.J. Fitzmartin, R.G. Gels, and E.J. Balboni, In *Optical Technology for Microwave Applications V* (USA, August 1991) p. 56. https://doi.org/10.1117/12.45560.
6. Q. H. Kareem, R. A. Shihab, and H. H. Kareem, Progress In Electromagnetics Research C, **137**, 185 (2023). https://doi.org/10.2528/PIERC23072204.
7. N. H. Biddut, M. E. Haque, and N. Jahan, In *2022 International Mobile and Embedded Technology Conference (MECON),* (India, Mar. 2022). P.113. https://doi.org/10.1109/mecon53876.2022.9751951.
8. K. Mazen, A. Emran, A. S. Shalaby, and A. Yahya, *International Journal of Advanced Computer Science and Applications*, **12**, 2021. https://doi.org/10.14569/IJACSA.2021.0120557

9. M. T. Ali, I. Aizat, I. Pasya, M. H. M. Zaharuddin, and N. Yaacob, in *IEEE International RF and Microwave Conference*, (Malaysia, 2011).https://doi.org/10.1109/RFM.2011.6168785.
10. D. Subitha, S. Velmurugan, and S. Balasubramani, in *Eighth International Conference New Trends In The Applications of Differential Equations in Sciences* (Ntades2021), AIP Publishing, 2022. https://doi.org/10.1063/5.0072473.
11. P. M. Teresa and G. Umamaheswari, IETE Journal of Research, **68**, 3778 (2020). https://doi.org/10.1080/03772063.2020.1779620.
12. M. S. H. Mollah, O. Faruk, M. S. Hossain, Md. T. Islam, A. S. M. Shafi, and M. M. I. Molla, *in 2021 IEEE 11th IEEE Symposium on Computer Applications &Amp; Industrial Electronics (ISCAIE)*, (Malaysia, Apr. 2021). p.343. https://doi.org/10.1109/iscaie51753.2021.9431793.
13. S.-E. Didi, I. Halkhams, M. Fattah, Y. Balboul, S. Mazer, and M. El Bekkali, TELKOMNIKA (Telecommunication Computing Electronics and Control), **20**, 527 (2020). https://doi.org/10.12928/telkomnika.v20i3.23159.
14. M.E. Godinez, C.S. McDermitt, A.S. Hastings, M.G. Parent, and F. Bucholtz, Journal of lightwave technology, **26**, 3829 (2008). https://doi.org/10.1109/JLT.2008.927794.
15. A. V. Kildishev, J. D. Borneman, K.-P. Chen, and V. P. Drachev, Sensors**, 11,** 717 (2011). https://doi.org/10.3390/s110707178.
16. Y. Ikeda and R. Tsuruoka, Applied Optics, **51,** 191 (2012). https://doi.org/10.1364/ao.51.00b183.
17. Y.-F. C. Chau, C.-T. C. Chao, J.-Y. Rao, H.-P. Chiang, C. M. Lim, R. C. Lim, and N. Y. Voo, Nanoscale Research Letters, **11**, 411 (2016). https://doi.org/10.1186/s11671-016-1606-9.
18. J. Hayashi, C. Liu, F. Akamatsu, A. Nishiyama, A. Moon, and Y. Ikeda, *in Proceedings of the International Conference on Ignition Systems for Gasoline Engines*, (Berlin, Germany, 2016).
19. R. Taubert, J. Dorfmüller, R. Vogelgesang, K. Kern, and H. Giessen, Nature Communications, **2,** 267 (2011). https://doi.org/10.1038/ncomms1268.
20. K. Holmberg and A. Matthews, *Coatings tribology: properties, mechanisms, techniques and applications in surface engineering*. Elsevier, 2009.
21. L. Novotny and N. van Hulst, Nature Photonics, **5**, 83 (2011). https://doi.org/10.1038/nphoton.2010.237.
22. C. W. Draper and P. Mazzoldi, *Laser surface treatment of metals*. Springer Science & Business Media, 2012.
23. S. Kaur, R. Khanna, P. Sahni, and N. Kumar, *International Journal of Innovative Technology and Exploring Engineering*, **8**, 611 (2019). https://doi.org/10.35940/ijitee.i1097.0789s19.
24. G. Casu, C. Moraru, and A. Kovacs, *in 2014 10th International Conference on Communications (COMM)*, (Romania, May 2014).p.1. https://doi.org/10.1109/iccomm.2014.6866738.
25. W. Hussain, International Journal of Engineering Works, **1**, 15 (2020). https://doi.org/10.34259/ijew.20.7011521.
26. X. Tang, Y. Jiao, H. Li, W. Zong, Z. Yao, F. Shan, Y. Li, W. Yue, and S. Gao, *in Proceedings of the 2019 International Workshop on Electromagnetics: Applications and Student Innovation Competition (iWEM)*, (Qingdao, China, 2019), p 5. https://doi.org/10.1109/iWEM45946.2019.
27. A. Kapoor, R. Mishra, A. Kapoor, and P. Kumar, International Journal of Smart Sensor and Intelligent Systems, **13**, 1 (2020). https://doi.org/10.21307/ijssis-2020-033.
28. L. C. Paul, S. C. Das, T. Rani, S. M. Muyeen, S. A. Shezan, and M. F. Ishraque, Heliyon, **8**, 12040 (2022). https://doi.org/10.1016/j.heliyon.2022.e12040.
29. S. K. Noor, M. Jusoh, T. Sabapathy, A. H. Rambe, H. Vettikalladi, A. M. Albishi, and M. Himdi, Electronics, **12,** 2555 (2023). https://doi.org/10.3390/electronics12122555.
30. A. H. Khidhir, Iraqi Journal of Science, **64,** 205 (2023). https://doi.org/10.24996/igs.2023.64.1.21.
31. A.H. Khidhir , Iraqi Journal of Physics:**18,** 17 (2020). https://doi.org/ 10.30723/ijp.18.44.17-24.
32. A.H. Khidhir, Iraqi Journal of Physics:**18**, 32(2020). https://doi.org/10.30723/ijp.18.45.32-39.
33. A.H.Khidhir, Baghdad Science Journal, **17**, 120 (2020). https://doi.org/10.21123/bsj.2020.17.1.0120.

تصميم وتنفيذ هوائي الرقعة للأجهزة المحمولة المعالجة باستخدام ليزرنديميوم-ياك لتحسين أدائها للوصلات اللاسلكية

سارة ياس خضير[1] و علي حسن خضر[1]
[1] قسم الفيزياء، كلية العلوم، جامعة بغداد، بغداد، العراق

الخلاصة

تقدم هذه الورقة تصميم وتنفيذ هوائي رقعي ميكروستريب على شكل حرف E للاتصالات اللاسلكية. يتميز الهوائي بعدة مزايا، منها صغر الحجم، وانخفاض الارتفاع، وسهولة التركيب، وخفة الوزن، وانخفاض تكلفة التصنيع. يعمل الهوائي بتردد 3.2 و3.4 جيجاهرتز، باستخدام ركيزة FR4 ذات ثابت عزل كهربائي 4.3 وسماكة 1.4 مم. يتضمن التصميم فتحتين متوازيتين لتعديل تيار الرقعة السطحية. يحقق الهوائي ذو الشكل E خسائر ارتداد تبلغ -13 ديسيبل و-16 ديسيبل عند ترددي التشغيل 3.2 و3.4 جيجاهرتز على التوالي. تم إجراء التصميم والمحاكاة باستخدام برنامج CST، مع استخدام تغذية بمسبار محوري. علاوة على ذلك، تبحث هذه الدراسة تأثير خشونة السطح على امتصاص خط الإشعاع للهوائي المُستخدم، والذي عُولج باستخدام ليزر Nd:YAG عن طريق قصف خط الإشعاع للهوائي المطلوب لتقليل خشونة السطح تدريجيًا، مما حسّن أداء الهوائي عند ترددات الرنين 3.2 و3.4 جيجاهرتز. بعد المعالجة، أظهر الهوائي خسائر ارتداد بلغت -15.7 ديسيبل و-20 ديسيبل عند 3.2 و3.4 جيجاهرتز على التوالي. تُبرز هذه الخصائص إمكانات الهوائي ذي الشكل E المقلوب المُعالج بليزر Nd:YAG في تحسين أداء أنظمة الاتصالات اللاسلكية.

الكلمات المفتاحيه: هوائي رقعي على شكل E، بلوتوث، ليزر Nd:YAG، الجيل الخامس، عرض النطاق الترددي.